Journal of Zhejiang University-SCIENCE A (Applied Physics & Engineering)
ISSN 1673-565X (Print); ISSN 1862-1775 (Online)
www.jzus.zju.edu.cn; www.springerlink.com
E-mail: jzus@zju.edu.cn

Microbial dynamics and performance in a microbial electrolysis cell-anaerobic membrane bioreactor*

Shu-wen DU[1], Chao SUN[2], A-qiang DING[1], Wei-wang CHEN[1],
Ming-jie ZHANG[1], Ran CHENG[1], Dong-lei WU[†‡1]

[1]*Department of Environmental Engineering, College of Environmental and Resource Sciences, Zhejiang University, Hangzhou 310027, China*

[2]*Shanghai SUS Environment Co., Ltd., Shanghai 201703, China*

[†]E-mail: wudl@zju.edu.cn

Received Jan. 8, 2019; Revision accepted May 24, 2019; Crosschecked June 12, 2019

Abstract: Membrane fouling restricts the wide application of anaerobic membrane bio-reactors (AnMBRs). In this study, a microbial electrolytic cell (MEC)-AnMBR biosystem was constructed to relieve membrane fouling. Total chemical oxygen demand (COD) removal efficiency and methane production in MEC-AnMBR were increased to 6.7% and 77.1%, respectively, in comparison to AnMBR. The membrane fouling of MEC-AnMBR was greatly lessened by the slower growth of extracellular polymeric substances (EPS) and soluble microbial products (SMP). High-throughput sequencing analysis showed that *Synergistaceae-uncultured* and *Thermovirga* were enriched in MEC-AnMBR, and *Thermovirga* was found as the key functional microorganism. These results indicated that MEC-AnMBR could simultaneously enhance the reactor efficiency and mitigate membrane fouling.

Key words: Microbial electrolytic cell-anaerobic membrane bio-reactor (MEC-AnMBR); Chemical oxygen demand (COD) removal efficiency; Methane production; Membrane fouling; Microbial mechanism
https://doi.org/10.1631/jzus.A1900009 **CLC number:** X703.1

1 Introduction

Generally, wastewater treatment processes are energy intensive. Aeration consumes much energy and thus anaerobic treatments are considered attractive for their comparative energy efficiency (Song et al., 2018; Sun et al., 2018a). Compared to traditional anaerobic treatments, the anaerobic membrane bioreactor (AnMBR) is much more efficient owing to its smaller space requirements, lower sludge loss, and higher biogas production (Li et al., 2017; Talvitie et al., 2017). However, membrane fouling always occurs in AnMBRs especially at high sludge concentrations, and this limits their wide application (Katuri et al., 2014; Wang et al., 2016).

Extracellular polymeric substances (EPS) and soluble microbial products (SMP) are produced by microorganisms with the similar components, mainly proteins and polysaccharides, and they are the main pollutants in membrane fouling in AnMBR. Gao et al. (2011) thought that high EPS concentration would increase viscosity and slow down the diffusion of dissolved oxygen, that affected the normal physiological activities in *zoogloea* and reduced the membranous flux. Lee et al. (2002) found that the accumulation of SMP increased the sludge viscosity which increased membrane resistance. However, frequent cleaning or direct replacement of membranes increased energy consumption and operating costs (Sun et al., 2018b). Efficient ways are, therefore, urgently needed for enhancing the efficiency of AnMBR and mitigating membrane fouling (Sun et al., 2018a).

‡ Corresponding author
* Project supported by the Zhejiang Provincial Key Science and Technology Project (No. 2015C03008), China
ORCID: Shu-wen DU, https://orcid.org/0000-0002-1681-3407

Bio-electrochemical systems (BESs) employ cells as biocatalysts to drive redox reactions on a solid electrode and are considered as promising wastewater treatment technology. The combination of BES and AnMBR has been shown to be a feasible way of mitigating membrane fouling (Cusick et al., 2011; Chen et al., 2014; Ding et al., 2018). Microbial fuel cells (MFCs) and microbial electrolytic cells (MECs) are two main types of BESs which can alleviate membrane fouling while recovering energy during sewage treatment processes (Steinbusch et al., 2010; Ren et al., 2014; Shoener et al., 2014). Tian et al. (2014) found that MFC-AnMBR could actually alleviate membrane fouling by neutralizing the charge on the sludge surface and promoting sludge reunification. In contrast to MFCs, MECs could generate biogas from biodegradable organics during the wastewater treatment process. So MEC-AnMBR offered a promising biotechnology to control membrane fouling which could also improve waste stabilization along with methanogenesis (Fu et al., 2010; Wang et al., 2011). Dhar et al. (2013) reported that AnMBRs as pretreatment of MECs were found to improve energy recovery and they confirmed that propionate was bio-transformed to acetate and hydrogen gas. Ding et al. (2018) explored the effect of degradation of organic pollutants and membrane fouling in MEC-AnMBR under different conditions and showed that the chemical oxygen demand (COD) removal rate reached a maximum with an applied voltage of 0.6 V, and it was almost 1.2 times higher than that without the application of voltage. However, these studies mainly focused on the detection of conventional indicators and the analysis of metabolites without in-depth exploration of the microbial community.

In this study, the feasibility of MEC-AnMBR system was investigated for simultaneous enhancement of reactor efficiency and to mitigate membrane fouling. AnMBR and MEC-AnMBR were operated with synthetic high strength wastewater containing organics for 35 d of continuous operation. The performance in terms of waste stabilization and methanogenesis was investigated. The characteristics of membrane fouling were simultaneously monitored. In addition, the dynamics of the microbial community of the cathode were analyzed through a high-throughput sequencing technique. The relationships among external electric field, reactor efficiency, and microbial community are discussed here to clarify the mechanism of membrane fouling alleviation.

2 Materials and methods

2.1 Reactor construction

The MEC-AnMBR was comprised of a single chambered MEC reactor made from plexiglass with an effective volume of 2.7 L. The cathode material was a titanium mesh with a built-in hollow fiber ultrafiltration membrane module. The anode material was carbon felt with an area of 13 cm×6 cm and the electrode spacing was about 5 cm. A lead wire from the anode and the cathode connected to the external power supply was used to control the applied voltage with a 10 Ω resistance set in an external circuit. The reactor was fed with continuous influent at the bottom, and the effluent was filtered through the membrane and then flowed out. Influent and effluent were controlled by a constant current pump. The change of the transmembrane pressure (TMP) was monitored by a pressure gauge. A hole was provided for gas collection at the top of the reactor and the generated biogas was collected in the gas sampling bag. The configuration of the reactor is shown in Fig. 1.

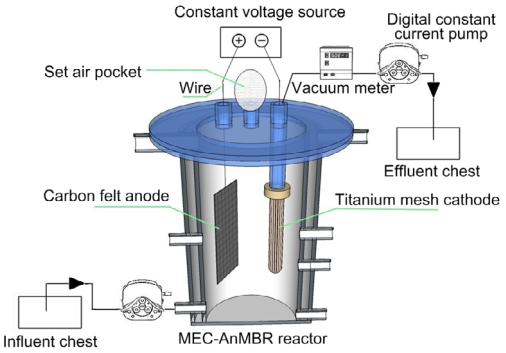

Fig. 1 Configuration of the MEC-AnMBR

2.2 Sludge and wastewater

The reactor was inoculated with secondary settling tank sludge from the Hangzhou Qige Sewage Treatment Plant, China.

The synthetic influent was high-concentration organic wastewater characterized by the COD concentration of 10 g/L. The composition of synthetic wastewater was as follows: CH_3COONa: 12.83 g/L;

NH_4Cl: 0.96 g/L; KH_2PO_4: 0.22 g/L; yeast extract: 0.1 g/L; tryptone: 0.1 g/L; trace elements solution: 1 mL/L. The trace element solution composition was administered according to previous study (Ding et al., 2018).

2.3 MEC-AnMBR membrane module

The membrane module for this experiment was provided by Tianjin MOTIMO Membrane Technology Co., Ltd., China. The membrane material was polyvinylidene fluoride (PVDF) and the membrane was in the form of an external pressure hollow fiber with a membrane pore diameter of 0.01 μm, the effective length of the membrane was 13 cm, the diameter of the filament was 1.2 mm, and the effective area was 0.1 m^2.

2.4 Reactor operation

The reactor was operated with a continuous constant flux inlet flow. The membrane flux was 0.56 L/(m^2·h) with a hydraulic retention time (HRT) of 2 d, and the volumetric loading was 4.8 kg COD/(m^3·d) operated at 28–30 °C in a constant temperature water bath.

A traditional AnMBR (open circuit) was operated as a control group, and the MEC-AnMBR (applied voltage of 0.8 V) was used as the experimental group. The operational period ended when the TMP reached 20 kPa; then a polluted membrane had to be replaced by a new one to maintain a steady operation.

2.5 Analyses and calculations

2.5.1 Analytical procedures

The influent COD concentration (COD_{in}), supernatant of reaction chamber (COD_{sup}) and of effluent (COD_{out}) were measured by the potassium dichromate method. COD removal efficiency was calculated as follows: The total COD (TCOD) removal efficiency (%)=[(COD_{in}−COD_{out})/COD_{in}] ×100%; The COD removal efficiency for the biodegradation (%)=[(COD_{in}−COD_{sup})/COD_{in}]×100%; The COD removal efficiency for the physical interception (%)=[(COD_{sup}−COD_{out})/COD_{in}]×100%. The TMP was obtained from the data from the vacuum gauge. The biogas production was measured by an indicating fermentation tube, and the biogenic components were analyzed by gas chromatography (GC9790, Fuli, China).

2.5.2 Analysis of microbial community

The biofilm was scraped from the bio-cathodes with a sterile scalpel. Genomic DNA was extracted from the two biofilm samples by the 3S DNA Isolation Kit (Bocai, China) according to the manufacturers' instructions and stored at −20 °C. One percent of agarose gel electrophoresis was used to test the integrity of genomic DNA. The bacterial 16S RNA gene was then amplified by GeneAmp PCR System (ABI Company, USA) using primers 338F (5'-ACTC CTACGGGAGGCAGCAG-3') and 806R (5'-GGAC TACHVGGGTWTCTAAT-3'). The archaeal 16S RNA gene was then amplified by GeneAmp PCR System (ABI Company, USA) using primers Arch344F (5'-ACGGGGYGCAGGCGCGA-3') and Arch915R (5'-GTGCTCCCCCGCCAATTCCT-3'). The PCR was conducted under the following conditions: 95 °C for 3 min, followed by 27 cycles at 95 °C for 30 s, 55 °C for 30 s, 72 °C for 45 s, and a final extension at 72 °C for 10 min. After the PCR product was purified and quantified, sequencing was performed on an Illumina Miseq PE250/PE300 platform (Majorbio Bio-Pharm Technology Co., Ltd., Shanghai, China). The paired-end (PE) readings obtained by Miseq sequencing were initially spliced according to the overlap relationship, and Trimmomatic and FLASH software were used to control the sequence quality and filter. Operational taxonomic units (OTU) clustering was performed using non-repetitive sequences according to 97% similarity, and the silva database was used as a reference database for subsequent analysis (Quast et al., 2013).

2.5.3 Scanning electron microscopy and confocal laser scanning microscope

Membrane silk was taken from the membrane module at the end of the membrane operational period according to a previously published protocol (Porras-Saavedra et al., 2018); finally it was observed under a scanning electron microscope (SEM) (FEI SIRION 0308947, the Netherlands) and a confocal laser scanning microscope (CLSM) (LSM780, Zeiss, Germany).

2.5.4 Analysis of EPS and SMP

The EPS and SMP of the sludge were removed by the heat extraction method. The sludge around the

membrane and on the membrane surface was obtained at the end of the membrane operational period, centrifuged for 10 min at 6000 r/min and the supernatant was removed. The residual sludge was mixed with deionized water. Continued centrifugation for 10 min at 6000 r/min, removed the supernatant and the centrifuge pellet was ground with 0.5% (w/v) NaCl solution. Then, 5 mL of the whole solution was put in a crucible (to measure the mixed liquid volatile suspended solids (MLVSS)) and the rest was heated in a thermostat water bath at 60 °C for 1 h, then centrifuged at 20000 r/min for 20 min. The supernatant (EPS sample) was collected and put in a refrigerator at 4 °C as reserve. The sludge sample (20 mL) was placed in a 50 mL centrifuge tube to centrifuge it for 10 min at 4000 r/min, the supernatant was filtered through a 0.45 μm filter, and the filtrate was the SMP sample. The protein content, including extracellular protein polymers (EPSp) and soluble microbial protein products (SMPp), was determined by the Folin-phenol method; the polysaccharide content, including extracellular polysaccharide polymers (EPSc) and soluble microbial polysaccharide products (SMPc), was determined by the phenol-sulfuric acid method.

3 Results and discussion

3.1 Performance of MEC-AnMBR

3.1.1 COD removal performance

The concentration of COD in reactor supernatant (sCOD) was basically stable and the COD removal rate gradually increased with the operation of the reactor (Fig. 2). At the end of the membrane operation, the TCOD removal efficiencies in AnMBR and MEC-AnMBR were 90.17% and 96.76%, respectively. The TCOD removal efficiency of MEC-AnMBR was obviously improved. The COD removal efficiency was mainly determined by the biological degradation of activated sludge and the physical retention of the membrane modules. In AnMBR, biodegradation accounted for 74.78% of the COD

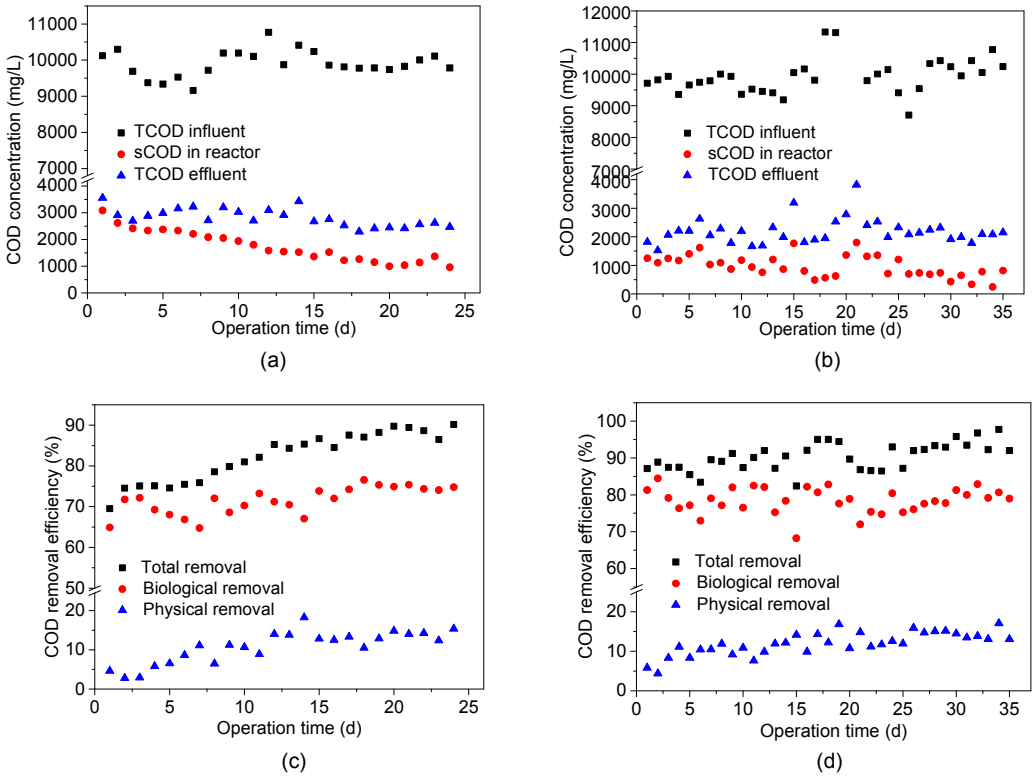

Fig. 2 COD concentrations in the influent, reactor supernatant, and effluent of AnMBR (a) and MEC-AnMBR (b), and the COD removal efficiencies in the influent, reactor supernatant, and effluent of AnMBR (c) and MEC-AnMBR (d)

removal efficiency, and physical retention accounted for 15.39%. In MEC-AnMBR, the proportion of biodegradation reached 82.92%, and the physical retention only accounted for 13.84%. Activated sludge plays an important role in COD removal during the whole operation compared with physical interception in the membrane module and this was due to the high microbial concentration and long sludge retention time (SRT) in the reactor which ensured efficient biodegradation of organic matter. The increase in COD removal mainly arose from biodegradation; the removal efficiency was stable during the membrane operational period in MEC-AnMBR (She et al., 2006; Sleutels et al., 2009; Ding et al., 2016). The addition of MECs strengthened the growth and microbial metabolism which eventually enhanced the COD removal performance (Baek and Pagilla, 2006; Ho and Sung, 2010; Nguyen et al., 2015).

3.1.2 Methane production performance

Biogas production indirectly reflects the reactor performance. The biogas produced in AnMBR and MEC-AnMBR includes CH_4, CO_2, H_2, and other gases, where the H_2 and CO_2 contents do not exceed 1% and 4%, respectively. As illustrated in Fig. 3, the methane concentration ranged between 80% and 95%. Methane production gradually increased from 2.5 L/d to 3.5 L/d in AnMBR, whereas it increased from 2.3 L/d up to 6.2 L/d in MEC-AnMBR. The methane concentration of MEC-AnMBR was significantly higher than that of AnMBR. It was mainly because the MECs provided the external electric field that could accelerate electron flow rate and significantly promote metabolic activity of the anaerobic methanogens on the cathode (Cheng et al., 2009; Clauwaert and Verstraete, 2009; Villano et al., 2010).

3.2 Membrane fouling

3.2.1 Characteristics of membrane fouling in MEC-AnMBR

Membrane fouling of AnMBR and MEC-AnMBR processes could be divided into three stages by observing the trend of TMP (Le-Clech et al., 2006). These were the initial stage, the cake formation stage, and the cake compaction stage (Fig. 4). TMP of AnMBR was 21.5 kPa on the 24th day while the TMP of the MEC-AnMBR reached 18 kPa in day 35. The membrane operational period of MEC-AnMBR was about 0.5 times longer than that of AnMBR, indicating that MEC-AnMBR could effectively alleviate membrane fouling. The images of the membrane module in each stage of membrane fouling in MEC-AnMBR are presented in Fig. 5. The biofilm surface gradually formed a dense cake layer with glaze microbial secretions, leading to more serious membrane fouling (Bagheri and Mirbagheri, 2018; Teng et al., 2018).

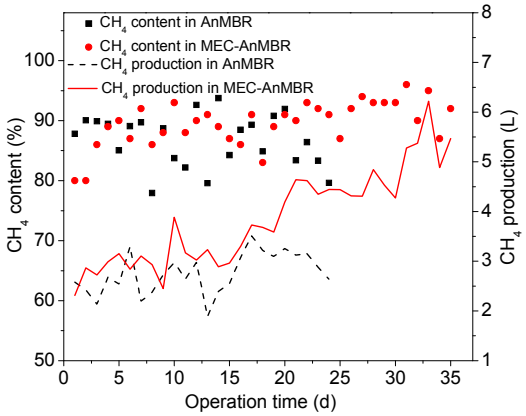

Fig. 3 CH_4 content and CH_4 production in AnMBR and MEC-AnMBR

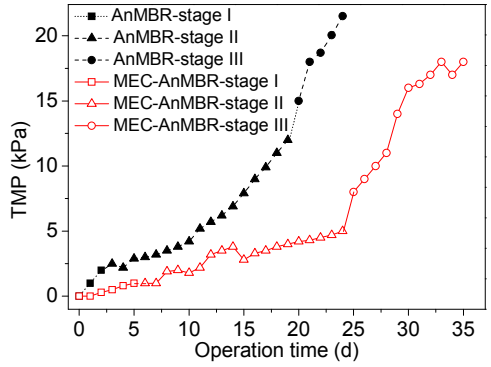

Fig. 4 TMP development with the membrane operational period in AnMBR and MEC-AnMBR

Akamatsu et al. (2010) succeeded in mitigating membrane fouling by application of an intermittent electric field to the membrane bioreactors. The membrane flux drastically reduced the static electricity generated by the intermittent electric field and peeling off the sludge from the membrane surface slowed down the membrane fouling. Tian et al. (2014) constructed an anaerobic membrane

bio-electrochemical reactor (AnEMBR) to treat low strength simulated wastewater by coupling an MEC and Ni-HFMs (hollow-fiber microfiltration). The membrane fouling of the AnEMBR was obviously alleviated by the hydrogen generated on the surface of the AnEMBR leading to a scouring effect at low cathodic potential and a local cathodic pH rise. Li et al. (2014) constructed a membrane bio-electrochemical reactor (MBER) along with MFC and MBR. It reduced membrane fouling from both the simulated wastewater and actual cheese plant wastewater (Li et al., 2014; Liu et al., 2018).

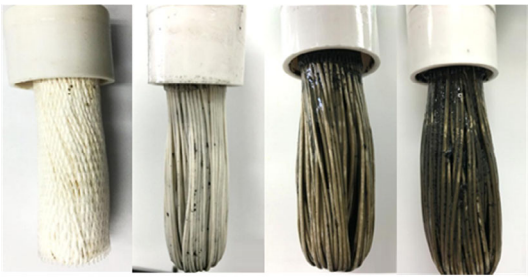

Fig. 5 Images of the membrane module in each stage of membrane fouling in MEC-AnMBR
(a) Before operation; (b) Initial membrane fouling stage; (c) Slow membrane fouling stage; (d) Rapid membrane fouling stage

3.2.2 Correlation of membrane fouling and reactor performance

The relationships between TMP and COD removal efficiency for both reactors are shown in Fig. 6. The increased membrane fouling was beneficial for the physical COD removal rate as it strengthened the physical retention of membrane components.

The methane production in AnMBR was not changed with the passage of time, while it gradually increased in MEC-AnMBR (Fig. 7). The increased methane production indicated a promoted methanogenic activity. At the same time, the higher gas production at the cathode had an eroding effect on the sludge around the membrane components, so membrane fouling was eased as well.

3.3 SEM image and CLSM analysis

The membrane module was taken from the reactor at the end of the operational period and a portion of the membrane was used for SEM. The comparison of the film surface in AnMBR and MEC-AnMBR is shown in Fig. 8; both of the film surfaces formed a dense cake layer with similar microbial morphologies.

The proteins and polysaccharides in microbial secretions seemed to be important sources of membrane fouling, because they could be easily adsorbed on the suspended sludge, the membrane surface, and the membrane pores, leading to membrane fouling. The fluorescence intensity of the labeled proteins and polysaccharides in MEC-AnMBR membranes was lower than that in AnMBR (Fig. 9), indicating that the concentrations of proteins and polysaccharides in MEC-AnMBR were lower.

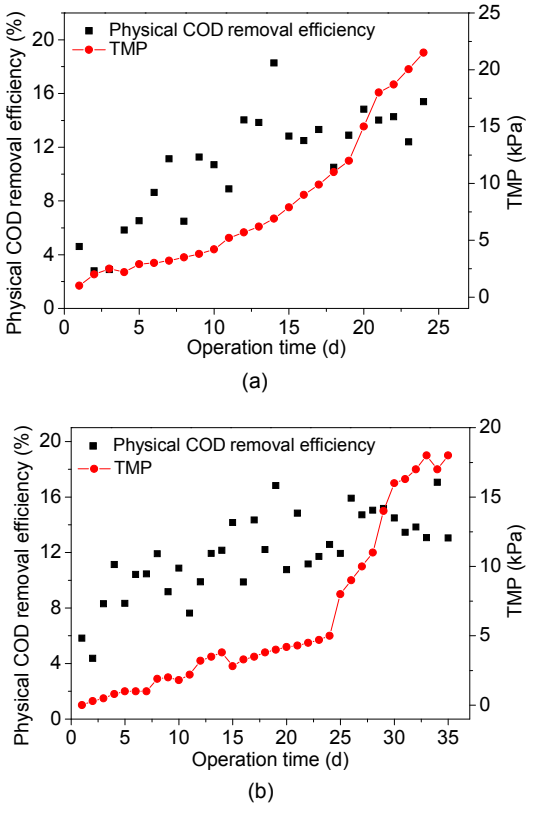

Fig. 6 TMP and physical COD removal efficiency developments with the membrane operational period of AnMBR (a) and MEC-AnMBR (b)

3.4 Microbial community analysis

In order to explore the mechanism of membrane fouling, the microbial communities belonging to archaea and bacteria on bio-cathodes were also analyzed in this study. Three membrane fouling stages

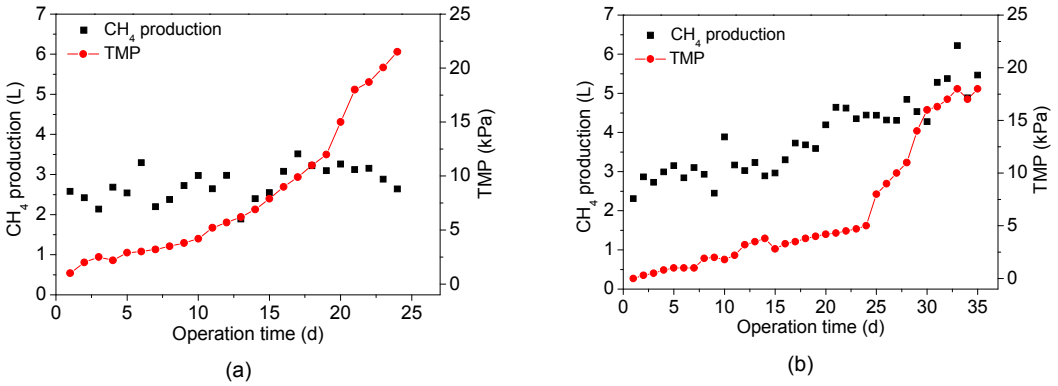

Fig. 7 TMP and CH_4 production development with the membrane operation time of AnMBR (a) and MEC-AnMBR (b)

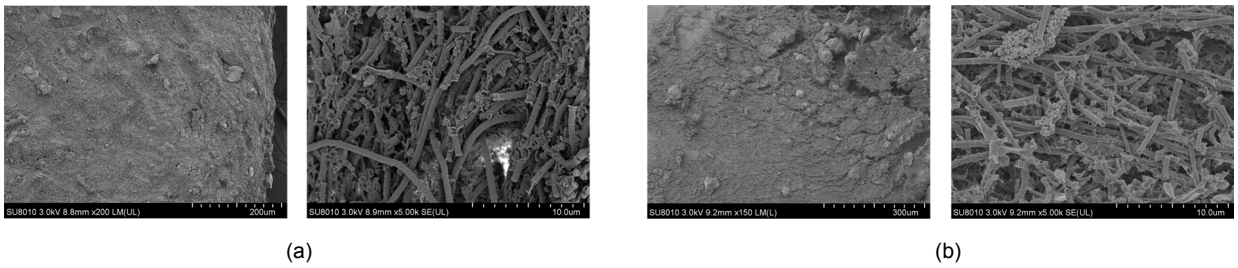

Fig. 8 SEM images of the membrane wire in AnMBR (a) and MEC-AnMBR (b)

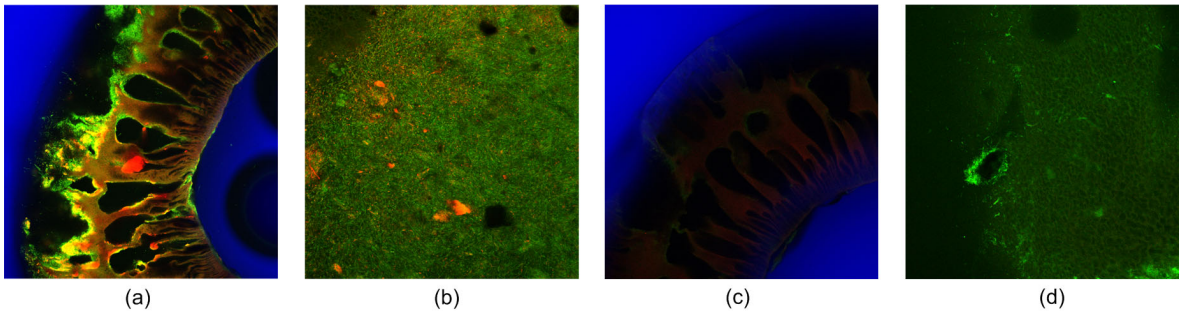

Fig. 9 CLSM images of the membrane of AnMBR and MEC-AnMBR

(a and c) CLSM images of a membrane section from AnMBR and MEC-AnMBR; (b and d) CLSM images of the membrane surface in AnMBR and MEC-AnMBR. Red indicates polysaccharide, while green indicates protein

in AnMBR were named as C-A-1, C-A-2, and C-A-3, respectively. These stages of MEC-AnMBR were correspondingly named as M-A-1, M-A-2, and M-A-3.

High-throughput sequencing was performed on archaea in the six samples of the traditional AnMBR and MEC-AnMBR for each membrane fouling stage, and 35 744, 38 400, 30 465, 33 480, 31 371, and 29 341 valid sequences were obtained, respectively. At 97% similarity, 21, 21, 14, 20, 13, and 15 OTUs could be generated by clustering. As listed in Table 1, the Shannon indices of the archaeal community increased in AnMBR but decreased in MEC-AnMBR during membrane operation. However, the value of MEC-AnMBR was higher than that of AnMBR.

The archaeal communities of both reactors were significantly different (Fig. 10a). *Methanosaeta* was the dominant genus in AnMBR while *Methanosarcina* was the dominant genus in MEC-AnMBR. In AnMBR *Methanosaeta* accounted for 93.74% and 94.08% during stages I and II, although it decreased

to 56.14% in stage III. In MEC-AnMBR the number of *Methanosarcina* was slightly higher than *Methanosaeta* during stages I and II, but in stage III, the relative abundance of *Methanosarcina* was much higher than *Methanosaeta*. The relative abundance of *Methanosarcina* increased during the anaerobic digestion which indicated that the environmental conditions in the MEC-AnMBR system were much more suitable for *Methanosarcina*. *Methanosaeta* is a strictly acetoclastic methanogen, while *Methanosarcina* can produce methane using all three methanogenesis pathways (acetoclastic, hydrogenotrophic, and methylotrophic methanogenesis) (Cheng et al., 2009; Clauwaert and Verstraete, 2009). In the MEC-AnMBR system, methane was primarily produced by methanogens through hydrogenotrophic methanogenesis with the reduction of CO_2 on the cathode by direct capture of electrons.

High-throughput sequencing was also performed on bacterial communities in AnMBR and MEC-AnMBR at each membrane fouling stage. Six groups of samples were respectively obtained 30326, 31690, 30358, 32123, 26185, and 31542 valid sequences, and 357, 360, 380, 371, 335, and 298 OTUs could be generated by clustering at 97% similarity level. As listed in Table 2, the Shannon indices of the bacteria community decreased in both AnMBR and MEC-AnMBR; however, there was no significant difference between the two reactors.

The bacterial genera in different samples are presented in Fig. 10b. The dominant genera were *Synergistaceae_uncultured* and *Thermovirga* in AnMBR and MEC-AnMBR during stage III and their percentages were 29.56% and 22.00%, respectively. *Thermovirga* was another dominant genus of the two reactors. The relative abundance of *Thermovirga* was 12.52% in AnMBR and 22.00% in MEC-AnMBR, which increased in both reactors during the degradation process. *Synergistaceae_uncultured* and *Thermovirga*, the long-chain fatty acid degrading anaerobic fermentative bacteria, are able to coexist with *methanobacteria* (Dahle and Birkeland, 2006). As a result, they were the dominant species in the anaerobic fermentation system. *Thermovirga* displayed high hydrolytic ability and had a high tolerance to highly saline wastewater (Wang et al., 2017). In the MEC-AnMBR system, *Thermovirga* accelerates hydrolysis and generates small molecules that can be utilized by *methanobacteria* to enhance methanogenesis.

Table 1 Richness and alpha-diversity of archaea in six samples

Sample	Readings	0.97 similarity level			
		OTU	Shannon	Simpson	Coverage
C-A-1	35744	21	0.35	0.8796	0.999944
C-A-2	38400	21	0.32	0.8864	0.999922
C-A-3	30465	14	0.86	0.4748	0.999934
M-A-1	33480	20	1.15	0.4121	0.999970
M-A-2	31371	13	0.92	0.4646	1.000000
M-A-3	29341	15	0.87	0.6286	0.999898

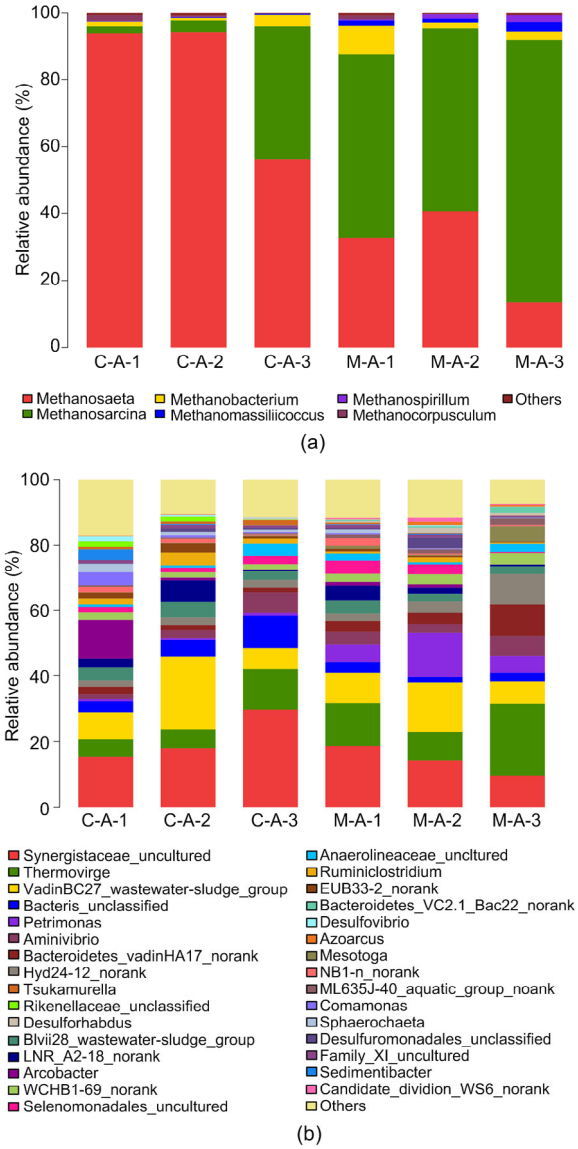

Fig. 10 Relative abundance of archaea (a) and bacteria (b) at the genus level in six samples

3.5 Mitigation mechanism of membrane fouling in MEC-AnMBR

To further reveal the mechanism of membrane fouling, the composition of EPSs and SMPs in suspended sludge and membrane surface sludge was measured for both reactors. Data analysis showed that EPSp and EPSc contents in the suspended sludge of MEC-AnMBR were higher during the membrane contamination stage.

It was evident that the EPSp and EPSc concentrations in AnMBR membrane sludge gradually increased with reactor operation, while the concentrations of EPSp and EPSc in the MEC-AnMBR did not change with the passage of time (Fig. 11). The EPSp and EPSc concentrations in the membrane surface sludge of MEC-AnMBR were higher than that of AnMBR during the initial stage but lower than that of AnMBR at the end. This may be due to the combination of the MEC that accelerated microbial electrons transport, leading to an elevation of microbial metabolic activity at the beginning of MEC-AnMBR, so that the EPSs content was significantly higher than that of AnMBR and it entered into the normal stage earlier (Zhang et al., 2009; Soler-Cabezas et al., 2018). The concentration of EPSp and EPSc rapidly increased with AnMBR operation. By comparison, the microbial metabolism and energy generation were strengthened under the influence of the MEC, as the microbes in MEC-AnMBR used more extracellular nutrients resulting in no increase of EPSp and EPSc during operation. Thus, the sludge would not subside and easily agglomerated on the membrane surface, which indicated that the growth rate of sludge cake layer was slow. At the end, the concentrations of EPSp and EPSc were significantly lower than that of AnMBR and the membrane fouling in MEC-AnMBR was alleviated (Zhang et al., 2017; Aslam et al., 2018).

During the initial period in MEC-AnMBR, the concentration of SMPp in the suspended sludge and membrane surface sludge was higher than that of AnMBR. The concentration of SMPp in AnMBR cathode film module gradually increased during the later stage and the concentration of SMPp in AnMBR cathode membrane module was significantly higher than that in MEC-AnMBR (Fig. 12). It could be attributed to the combination of MEC in AnMBR; the microbial metabolism in the reactor was enhanced with significantly high SMPp concentration in AnMBR. However, the SMPp concentration did not significantly fluctuate in MEC-AnMBR. The concentration of SMPp in MEC-AnMBR was

Table 2 Richness and alpha-diversity of bacteria in six samples

Sample	Readings	0.97 similarity level			
		OTU	Shannon	Simpson	Coverage
C-A-1	30326	357	4.08	0.0393	0.998714
C-A-2	31690	360	3.71	0.0525	0.998454
C-A-3	30358	380	3.68	0.0609	0.998089
M-A-1	32123	371	3.88	0.0461	0.998693
M-A-2	26185	335	3.70	0.0524	0.997709
M-A-3	31542	298	3.36	0.0812	0.998447

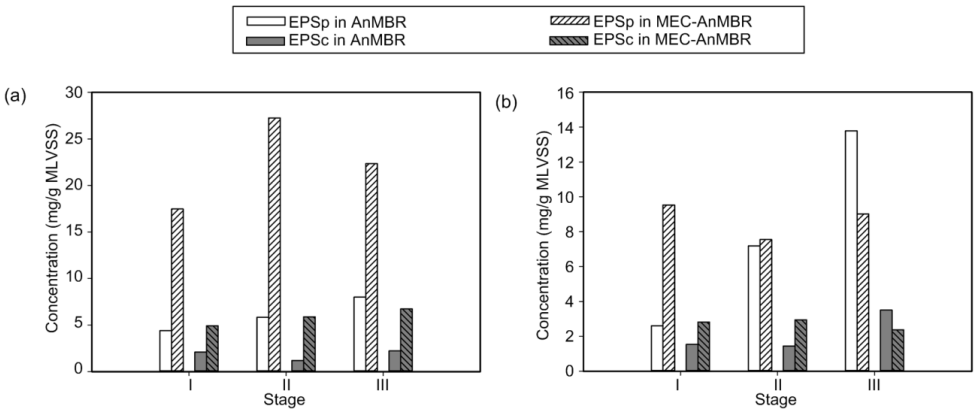

Fig. 11 Concentrations of EPSp and EPSc in the suspended sludge (a) and membrane surface sludge (b) of AnMBR and MEC-AnMBR

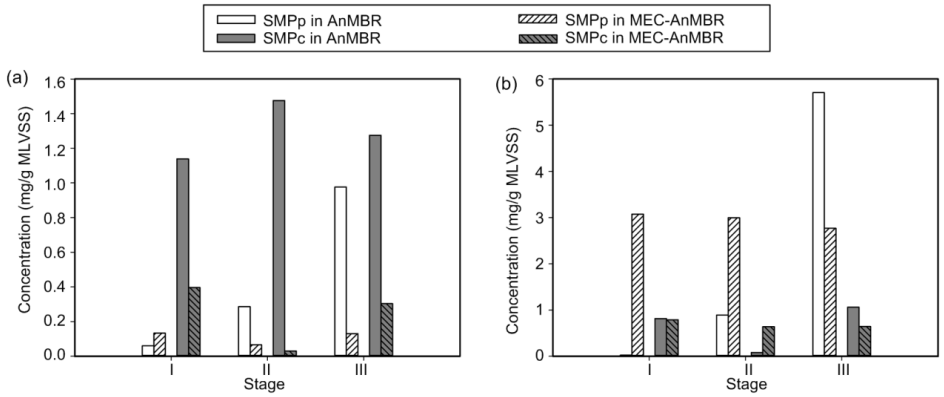

Fig. 12 Concentrations of SMPp and SMPc in the suspended sludge (a) and membrane surface sludge (b) of AnMBR and MEC-AnMBR

significantly lower than that in AnMBR during the later stage of operation. The concentration of SMPc in AnMBR and MEC-AnMBR membrane sludge was relatively low and varied slightly during the operation. Studies have shown that a large accumulation of EPS and SMP in the suspended sludge and membrane surface sludge can aggravate membrane fouling (Zhu et al., 2018). Therefore, MEC-AnMBRs could reduce membrane fouling by reducing the growth rates of EPS and SMPp concentrations (Lee et al., 2002; Gao et al., 2004).

4 Conclusions

In the current study, the successful establishment of MEC-AnMBR could effectively alleviate membrane fouling and improve the reactor efficiency. The maximum COD removal efficiency of MEC-AnMBR was around 96.8% and the methane production was 6.2 L/d. The membrane operational period was extended to 35 d compared with AnMBR (24 d). *Thermovirga* and *Methanosarcina* were inferred to be the key functional microorganisms in MEC-AnMBR. The slow growth rates of ESP and SMP in the membrane surface sludge were the primary reason for membrane fouling mitigation.

Contributors

Shu-wen DU wrote the first draft of the manuscript and edited the final version. Chao SUN formulated research goals and revised the manuscript. A-qiang DING provided experimental resources. Wei-wang CHEN conducted a research and investigation process. Ming-jie ZHANG created models. Ran CHENG analyzed the data. Dong-lei WU oversaw and led the research activity.

Conflict of interest

Shu-wen DU, Chao SUN, A-qiang DING, Wei-wang CHEN, Ming-jie ZHANG, Ran CHENG, and Dong-lei WU declare that they have no conflict of interest.

References

Akamatsu K, Lu W, Sugawara T, et al., 2010. Development of a novel fouling suppression system in membrane bioreactors using an intermittent electric field. *Water Research*, 44(3):825-830. https://doi.org/10.1016/j.watres.2009.10.026

Aslam M, Yang PX, Lee PH, et al., 2018. Novel staged anaerobic fluidized bed ceramic membrane bioreactor: energy reduction, fouling control and microbial characterization. *Journal of Membrane Science*, 553:200-208. https://doi.org/10.1016/j.memsci.2018.02.038

Baek SH, Pagilla KR, 2006. Aerobic and anaerobic membrane bioreactors for municipal wastewater treatment. *Water Environment Research*, 78(2):133-140. https://doi.org/10.2175/106143005X89599

Bagheri M, Mirbagheri SA, 2018. Critical review of fouling mitigation strategies in membrane bioreactors treating water and wastewater. *Bioresource Technology*, 258: 318-334. https://doi.org/10.1016/j.biortech.2018.03.026

Chen JY, Li N, Zhao L, 2014. Three-dimensional electrode microbial fuel cell for hydrogen peroxide synthesis coupled to wastewater treatment. *Journal of Power Sources*, 254:316-322. https://doi.org/10.1016/j.jpowsour.2013.12.114

Cheng SA, Xing DF, Call DF, et al., 2009. Direct biological conversion of electrical current into methane by electromethanogenesis. *Environmental Science & Technology*, 43(10):3953-3958. https://doi.org/10.1021/es803531g

Clauwaert P, Verstraete W, 2009. Methanogenesis in membraneless microbial electrolysis cells. *Applied Microbiology and Biotechnology*, 82(5):829-836. https://doi.org/10.1007/s00253-008-1796-4

Cusick RD, Bryan B, Parker DS, et al., 2011. Performance of a pilot-scale continuous flow microbial electrolysis cell fed winery wastewater. *Applied Microbiology and Biotechnology*, 89(6):2053-2063. https://doi.org/10.1007/s00253-011-3130-9

Dahle H, Birkeland NK, 2006. *Thermovirga lienii gen. nov., sp. nov*., a novel moderately thermophilic, anaerobic, amino-acid-degrading bacterium isolated from a North Sea oil well. *International Journal of Systematic and Evolutionary Microbiology*, 56(7):1539-1545. https://doi.org/10.1099/ijs.0.63894-0

Dhar BR, Gao YH, Yeo H, et al., 2013. Separation of competitive microorganisms using anaerobic membrane bioreactors as pretreatment to microbial electrochemical cells. *Bioresource Technology*, 148:208-214. https://doi.org/10.1016/j.biortech.2013.08.138

Ding AQ, Yang Y, Sun GD, et al., 2016. Impact of applied voltage on methane generation and microbial activities in an anaerobic microbial electrolysis cell (MEC). *Chemical Engineering Journal*, 283:260-265. https://doi.org/10.1016/j.cej.2015.07.054

Ding AQ, Fan Q, Cheng R, et al., 2018. Impacts of applied voltage on microbial electrolysis cell-anaerobic membrane bioreactor (MEC-AnMBR) and its membrane fouling mitigation mechanism. *Chemical Engineering Journal*, 333:630-635. https://doi.org/10.1016/j.cej.2017.09.190

Fu L, You SJ, Yang FL, et al., 2010. Synthesis of hydrogen peroxide in microbial fuel cell. *Journal of Chemical Technology & Biotechnology*, 85(5):715-719. https://doi.org/10.1002/jctb.2367

Gao MC, Yang M, Li HY, et al., 2004. Nitrification and sludge characteristics in a submerged membrane bioreactor on synthetic inorganic wastewater. *Desalination*, 170(2): 177-185. https://doi.org/10.1016/j.desal.2004.02.099

Gao WJ, Lin HJ, Leung KT, et al., 2011. Structure of cake layer in a submerged anaerobic membrane bioreactor. *Journal of Membrane Science*, 374(1-2):110-120. https://doi.org/10.1016/j.memsci.2011.03.019

Ho J, Sung S, 2010. Methanogenic activities in anaerobic membrane bioreactors (AnMBR) treating synthetic municipal wastewater. *Bioresource Technology*, 101(7): 2191-2196. https://doi.org/10.1016/j.biortech.2009.11.042

Katuri KP, Werner CM, Jimenez-Sandoval RJ, et al., 2014. A novel anaerobic electrochemical membrane bioreactor (AnEMBR) with conductive hollow-fiber membrane for treatment of low-organic strength solutions. *Environmental Science & Technology*, 48(21):12833-12841. https://doi.org/10.1021/es504392n

Le-Clech P, Chen V, Fane TAG, 2006. Fouling in membrane bioreactors used in wastewater treatment. *Journal of Membrane Science*, 284(1-2):17-53. https://doi.org/10.1016/j.memsci.2006.08.019

Lee Y, Cho J, Seo Y, et al., 2002. Modeling of submerged membrane bioreactor process for wastewater treatment. *Desalination*, 146(1-3):451-457. https://doi.org/10.1016/S0011-9164(02)00543-X

Li HN, He WH, Qu YP, et al., 2017. Pilot-scale benthic microbial electrochemical system (BMES) for the bioremediation of polluted river sediment. *Journal of Power Sources*, 356:430-437. https://doi.org/10.1016/j.jpowsour.2017.03.066

Li J, Ge Z, He Z, 2014. Advancing membrane bioelectrochemical reactor (MBER) with hollow-fiber membranes installed in the cathode compartment. *Journal of Chemical Technology & Biotechnology*, 89(9):1330-1336. https://doi.org/10.1002/jctb.4206

Liu JD, Xiong JX, Tian C, et al., 2018. The degradation of methyl orange and membrane fouling behavior in anaerobic baffled membrane bioreactor. *Chemical Engineering Journal*, 338:719-725. https://doi.org/10.1016/j.cej.2018.01.052

Nagaoka H, Ueda S, Miya A, 1996. Influence of bacterial extracellular polymers on the membrane separation activated sludge process. *Water Science and Technology*, 34(9):165-172. https://doi.org/10.1016/S0273-1223(96)00800-1

Nguyen VK, Hong S, Park Y, et al., 2015. Autotrophic denitrification performance and bacterial community at biocathodes of bioelectrochemical systems with either abiotic or biotic anodes. *Journal of Bioscience and Bioengineering*, 119(2):180-187. https://doi.org/10.1016/j.jbiosc.2014.06.016

Porras-Saavedra J, Alamilla-Beltrán L, Lartundo-Rojas L, et al., 2018. Chemical components distribution and morphology of microcapsules of paprika oleoresin by microscopy and spectroscopy. *Food Hydrocolloids*, 81: 6-14. https://doi.org/10.1016/j.foodhyd.2018.02.005

Quast C, Pruesse E, Yilmaz P, et al., 2013. The SILVA ribosomal RNA gene database project: improved data processing and web-based tools. *Nucleic Acids Research*, 41(D1):D590-D596. https://doi.org/10.1093/nar/gks1219

Ren LJ, Ahn Y, Logan BE, 2014. A two-stage microbial fuel cell and anaerobic fluidized bed membrane bioreactor (MFC-AFMBR) system for effective domestic wastewater treatment. *Environmental Science & Technology*, 48(7):4199-4206. https://doi.org/10.1021/es500737m

She P, Song B, Xing XH, et al., 2006. Electrolytic stimulation of bacteria *Enterobacter dissolvens* by a direct current. *Biochemical Engineering Journal*, 28(1):23-29. https://doi.org/10.1016/j.bej.2005.08.033

Shoener BD, Bradley IM, Cusick RD, et al., 2014. Energy positive domestic wastewater treatment: the roles of

anaerobic and phototrophic technologies. *Environmental Science: Processes & Impacts*, 16(6):1204-1222. https://doi.org/10.1039/C3EM00711A

Sleutels THJA, Hamelers HVM, Rozendal RA, et al., 2009. Ion transport resistance in microbial electrolysis cells with anion and cation exchange membranes. *International Journal of Hydrogen Energy*, 34(9):3612-3620. https://doi.org/10.1016/j.ijhydene.2009.03.004

Soler-Cabezas JL, Luján-Facundo MJ, Mendoza-Roca JA, et al., 2018. A comparative study of the influence of salt concentration on the performance of an osmotic membrane bioreactor and a sequencing batch reactor. *Journal of Chemical Technology & Biotechnology*, 93(1):72-79. https://doi.org/10.1002/jctb.5321

Song XY, Luo WH, McDonald J, et al., 2018. An anaerobic membrane bioreactor–membrane distillation hybrid system for energy recovery and water reuse: removal performance of organic carbon, nutrients, and trace organic contaminants. *Science of the Total Environment*, 628-629:358-365. https://doi.org/10.1016/j.scitotenv.2018.02.057

Steinbusch KJJ, Hamelers HVM, Schaap JD, et al., 2010. Bioelectrochemical ethanol production through mediated acetate reduction by mixed cultures. *Environmental Science & Technology*, 44(1):513-517. https://doi.org/10.1021/es902371e

Sun L, Tian Y, Zhang J, et al., 2018a. Wastewater treatment and membrane fouling with algal-activated sludge culture in a novel membrane bioreactor: influence of inoculation ratios. *Chemical Engineering Journal*, 343:455-459. https://doi.org/10.1016/j.cej.2018.03.022

Sun L, Tian Y, Zhang J, et al., 2018b. A novel symbiotic system combining algae and sludge membrane bioreactor technology for wastewater treatment and membrane fouling mitigation: performance and mechanism. *Chemical Engineering Journal*, 344:246-253. https://doi.org/10.1016/j.cej.2018.03.090

Talvitie J, Mikola A, Koistinen A, et al., 2017. Solutions to microplastic pollution–removal of microplastics from wastewater effluent with advanced wastewater treatment technologies. *Water Research*, 123:401-407. https://doi.org/10.1016/j.watres.2017.07.005

Teng JH, Shen LG, Yu GY, et al., 2018. Mechanism analyses of high specific filtration resistance of gel and roles of gel elasticity related with membrane fouling in a membrane bioreactor. *Bioresource Technology*, 257:39-46. https://doi.org/10.1016/j.biortech.2018.02.067

Tian Y, Ji C, Wang K, et al., 2014. Assessment of an anaerobic membrane bio-electrochemical reactor (AnMBER) for wastewater treatment and energy recovery. *Journal of Membrane Science*, 450:242-248. https://doi.org/10.1016/j.memsci.2013.09.013

Villano M, Aulenta F, Ciucci C, et al., 2010. Bioelectrochemical reduction of CO_2 to CH_4 via direct and indirect extracellular electron transfer by a hydrogenophilic methanogenic culture. *Bioresource Technology*, 101(9):3085-3090. https://doi.org/10.1016/j.biortech.2009.12.077

Wang J, Bi FH, Ngo HH, et al., 2016. Evaluation of energy-distribution of a hybrid microbial fuel cell–membrane bioreactor (MFC–MBR) for cost-effective wastewater treatment. *Bioresource Technology*, 200:420-425. https://doi.org/10.1016/j.biortech.2015.10.042

Wang SJ, Hou XC, Su HJ, 2017. Exploration of the relationship between biogas production and microbial community under high salinity conditions. *Science Report*, 7:1149. https://doi.org/10.1038/s41598-017-01298-y

Wang YK, Sheng GP, Li WW, et al., 2011. Development of a novel bioelectrochemical membrane reactor for wastewater treatment. *Environmental Science & Technology*, 45(21):9256-9261. https://doi.org/10.1021/es2019803

Zhang HM, Xia J, Yang Y, et al., 2009. Mechanism of calcium mitigating membrane fouling in submerged membrane bioreactors. *Journal of Environmental Sciences*, 21(8):1066-1073. https://doi.org/10.1016/S1001-0742(08)62383-9

Zhang HM, Jiang W, Cui HT, 2017. Performance of anaerobic forward osmosis membrane bioreactor coupled with microbial electrolysis cell (AnOMEBR) for energy recovery and membrane fouling alleviation. *Chemical Engineering Journal*, 321:375-383. https://doi.org/10.1016/j.cej.2017.03.134

Zhu YJ, Wang YY, Zhou S, et al., 2018. Robust performance of a membrane bioreactor for removing antibiotic resistance genes exposed to antibiotics: role of membrane foulants. *Water Research*, 130:139-150. https://doi.org/10.1016/j.watres.2017.11.067

中文概要

题　目：微生物电解池耦合厌氧膜生物反应器运行性能及微生物学机理研究

目　的：将微生物电解池（MEC）与厌氧膜生物反应器（AnMBR）耦合，构建 MEC-AnMBR 系统，以期同步实现污水高效处理和膜污染缓解，推动膜生物反应器的理论创新和技术创新。

创新点：1. 将 MEC 与 AnMBR 耦合，构建 MEC-AnMBR 系统用于高浓度有机废水的处理；2. 研究反应器运行和微生物群落之间的关系；3. 探究膜污染运行周期中各膜污染阶段微生物代谢产物与自身代谢活性的变化规律。

方　法：1. 启动和运行 MEC-AnMBR 反应器，并与传统 AnMBR 对照，综合考察 MEC-AnMBR 反应器的运行性能；2. 利用高通量测序技术对传统 AnMBR 和 MEC-AnMBR 各膜污染阶段的阴极膜表面微生物群落结构及多样性进行研究，并综合

分析 MEC-AnMBR 反应器的运行特性与微生物群落间的相互关系；3. 对 MEC-AnMBR 反应器阴极膜组件及微生物分泌物进行原位观察，并研究其在膜污染运行周期中各膜污染阶段微生物代谢产物与自身代谢活性的变化规律。

结　论：1. 成功构建微生物电解池 MEC-AnMBR 生物系统；2. 与 AnMBR 相比，MEC-AnMBR 中的化学需氧量（COD）去除效率和甲烷产量分别增加 6.7%和 77.1%；3. 与 AnMBR 相比，MEC-AnMBR 的膜污染因细胞外聚合物和可溶性微生物产物增长缓慢而大大减少；4. 高通量测序分析表明 MEC-AnMBR 富含互养菌属（*Synergistaceae-uncultured*）和互营热菌属（*Thermovirga*），而 *Thermovirga* 是关键的功能性微生物；5. 这些结果表明 MEC-AnMBR 可同时提高反应器效率并减轻膜污染。

关键词：微生物电解池；COD 去除效率；甲烷产量；膜污染；微生物特性